Laser Process Proximity Correction for Improvement of Critical Dimension Linearity on a Photomask

Jong Rak Park, Hyun Su Kim, Jin-Tae Kim, Moon-Gyu Sung, Won-Il Cho, Ji-Hyun Choi, and Sung-Woon Choi

We report on the improvement of critical dimension (CD) linearity on a photomask by applying the concept of process proximity correction to a laser lithographic process used for the fabrication of photomasks. Rule-based laser process proximity correction (LPC) was performed using an automated optical proximity correction tool and we obtained dramatic improvement of CD linearity on a photomask. A study on model-based LPC was executed using a two-Gaussian kernel function and we extracted model parameters for the laser lithographic process by fitting the model-predicted CD linearity data with measured ones. Model-predicted bias values of isolated space (I/S), arrayed contact (A/C) and isolated contact (I/C) were in good agreement with those obtained by the nonlinear curve-fitting method used for the rule-based LPC.

Keywords: Laser lithography, photomask fabrication, critical dimension linearity, process proximity correction.

Manuscript received June 15, 2004; revised Dec. 2, 2004.

Jong Rak Park (phone: + 82 62 230 7036, email: ejrpark@chosun.ac.kr), Hyun Su Kim (email: hskim21@chosun.ac.kr), and Jin-Tae Kim (email: kimjt@chosun.ac.kr) are with Department of Photonic Engineering, Chosun University, Gwangju, Korea.

Moon-Gyu Sung (email: cameleon.sung@samsung.com), Won-Il Cho (email: chowonil@samsung.com), Ji-Hyun Choi (email: prom.choi@samsung.com), and Sung-Woon Choi (email: cjiwoo@samsung.com) are with Photomask Team, Samsung Electronics Co., Ltd., Yongin, Korea.

I. Introduction

As the feature size for device manufacturing is ever decreasing, the requirements for minimum resolution on photomasks are becoming tighter and tighter [1]. Efforts to improve the patterning performance on photomasks can be tried from following three different aspects: mask pattern generators with higher resolution [2], new materials such as photomask blanks with thinner film thickness to reduce micro-loading effects in the dry-etch process [3], and mask process proximity correction.

Proximity correction is a compensation method of linewidth variation caused by a proximity effect that refers to features with the same nominal critical dimension (CD) printing differently due to environmental situations [4]. In particular, the correction applied to the proximity effect occurring in a projection imaging process is called optical proximity correction (OPC). Owing to the successful mathematical modeling of the projection imaging process, model-based methods based on optical lithography simulation tools are widely employed [5]-[7]. Nowadays, OPC is used for the correction of almost all kinds of image distortions including CD nonlinearity, line-end shortening, and corner rounding, as well as proximity effect, and is even applied to the correction of linewidth variation caused by non-optical origins, i.e., the post-imaging pattern transfer processes. In order to refer to the correction of the process proximity effect separately from that of the optical proximity effect, the terminology of process proximity correction (PPC) was introduced and is being widely used in the semiconductor manufacturing society [8].

Recently, loading effect correction (LEC) has been extensively studied [9]. LEC is a correcting method of pattern

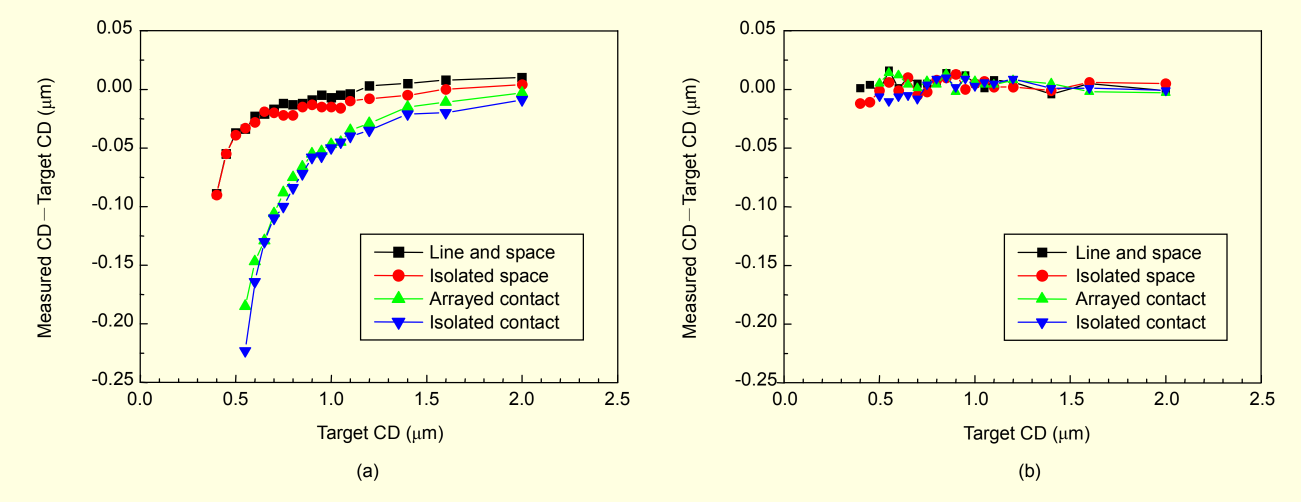

Fig. 1. CD linearity data measured (a) before rule-based LPC and (b) after rule-based LPC.

density dependent CD variation that mainly occurs at the dry-etch process step. The typical range of the dry-etch loading effect is in the order of millimeters, which indicates that LEC is addressing a somewhat global CD uniformity issue. Since the ranges of physical effects that can be coped with an OPC tool are limited, LEC cannot be performed using a typical OPC tool. Therefore, LEC is usually performed separately from and next to the OPC in the data preparation flow.

In this paper, we applied the PPC concept to the mask-making process of a laser pattern generator. The main concern of this paper is improving patterning resolution by applying the PPC concept to the mask-making process. Therefore, we have concentrated on the CD linearity issue rather than on the CD uniformity issue. In section II, we describe rule-based laser process proximity correction (LPC) using an automated OPC tool and report on the improvement of CD linearity on a photomask. In section III, the results of a preliminary study on model-based LPC using a two-Gaussian kernel function are presented. Finally, we conclude with a brief summary in section IV.

II. Rule-Based LPC

We first describe the mask-making process to which rule-based LPC was applied. An ALTA3700 (Etec) equipped with a 364-nm laser source and a binary mask coated with photoresist IP3500 (TOK) were used as a mask pattern generator and mask blank, respectively. The Samsung standard wet process for the photoresist IP3500 was used for the development process, and a dry-etch process was performed using plasma etch system VLR-Gen1 (Unaxis). The CD values reported below are chromium CDs in μm and are measured after the dry-etching and cleaning processes. The target CDs of the test patterns, which include 1:1 line-and-space (L/S), isolated space (I/S), 1:1 arrayed contact (A/C), and isolated contact (I/C) patterns, were varied from 0.4 to 2.0 μm in their sizes on a photomask, which corresponds to 0.1 to 0.5 μm feature sizes on a wafer. The design CDs of the test patterns were chosen to be 0.1 μm smaller than the target CDs to compensate for the known follow-up dry-etch bias.

Figure 1(a) shows the CD linearity data (differences between measured CDs and target CDs) measured before the rule-based LPC. We can see that contact-type patterns are more susceptible to patterning errors. CD linearity for L/S and I/S becomes deteriorated from about 0.5 μm in size, and that for A/C and I/C even earlier from about 1.0 μm in size. Although dense patterns (L/S and A/C) seem to be slightly better than isolated patterns (I/S and I/C) in their CD linearity characteristics, L/S and I/S, and A/C and I/C, respectively, show similar tendencies, which indicates that CD linearity is more dependent on pattern type than on pattern density with a decreasing target CD. In terms of the proximity effect, it can be said that for the mask-making process considered in this paper, the intra-pattern proximity effect is more dominant than inter-pattern proximity effect.

In order to extract bias rules for rule-based LPC, the curve-fitting method with a nonlinear function was used. The form of the nonlinear function is

$$M_{CD} = D_{CD} + a_1\left(D_{CD} - a_2\right)^{a_3} + a_4, \tag{1}$$

where M_{CD} and D_{CD} represent the measured CD and the design CD, respectively, and a_i's (i = 1, 2, 3, 4) are fitting parameters. Given that we have a functional relationship between M_{CD} and D_{CD} ($M_{CD} = f(D_{CD})$), by utilizing the inverse function of the relationship ($D_{CD} = f^{-1}(M_{CD})$), modified design CDs, with

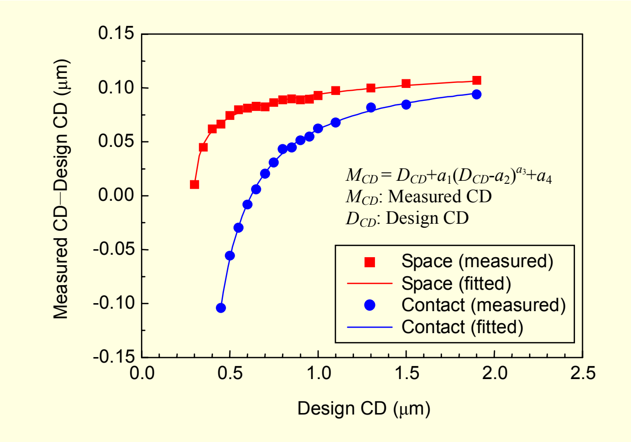

Fig. 2. Nonlinear curve-fitting results of CD skew data for space- and contact-type patterns.

which target CDs will be accomplished, can be easily calculated, and bias values for patterns on a design layout are therefore readily obtained. Since the patterns of a same type (space or contact) have similar CD linearity characteristics, we decided to apply one bias rule table to each (space or contact) pattern type. Figure 2 shows the results of the nonlinear curve-fitting. In Fig. 2, the measured values of space (contact) patterns refer to the average values for L/S and I/S (A/C and I/C) patterns. The fitting parameters for space and contact patterns were a_1 = –0.0903, a_2 = 0.2830, a_3 = –0.1681, a_4 = 0.1896 and a_1 = –0.0471, a_2 = 0.2508, a_3 = –0.9742, a_4 = 0.1237, respectively.

We used an automated OPC tool, Photolynx OPC Tek Editor (Synopsys, Inc.) for rule-based LPC. Bias rules for space and contact type patterns were tabulated using Photolynx OPC Tek Editor, and modification of the design layout for the test patterns was executed on the platform of a software package for photomask manufacturing data preparation, CATS (Synopsys, Inc.), with a 5 nm design grid. CD linearity data measured after rule-based LPC are depicted in Fig. 1(b). The CD linearity data were dramatically improved, and the differences between measured CDs and target CDs were within 25 nm for all test patterns. Since the CD nonlinearity problem is severer for contact-type patterns, we are trying to apply the rule-based LPC to a layout having contact-hole type patterns used for the manufacturing of real devices.

III. Model-Based LPC

In order to correct various kinds of pattern distortions in diverse environmental situations, considerable efforts are needed to extract correction rules for rule-based proximity correction. However, if one could determine a correction model that describes the patterning process completely, a model-based approach is much more preferable. There are two kinds of model-based proximity correction: one is based on the physical modeling of the patterning process and the other is based on the convolution of kernel functions and mask design layout. Physical modeling of all processes related with device patterning is an enormous and extremely difficult task. In particular, the dry-etching process is known to be the most difficult part to be physically modeled [10]. In this section, we attempt model-based LPC based on a kernel function. Recently, it was reported that the corner rounding of patterns on a photomask induced by the proximity effect in the mask-making process could be modeled with a one-Gaussian point spread function (PSF), and a modified mask layout using the one-Gaussian PSF was proven to produce more realistic results of a wafer patterning simulation than the unmodified original CAD layout [11]. In this section, we present the results of a preliminary study on model-based LPC using a two-Gaussian kernel.

The two-Gaussian kernel used for the model-based LPC is as follows:

$$K(r) = \frac{1}{\pi\alpha^2}\exp\left(-\frac{r^2}{\alpha^2}\right) + \frac{\eta}{\pi\beta^2}\exp\left(-\frac{r^2}{\beta^2}\right), \qquad (2)$$

$$r = \sqrt{x^2 + y^2},$$

where α, β and η represent a short kernel range, a long kernel range, and the ratio of long-range over short-range contribution, respectively, and x and y are mutually orthogonal Cartesian coordinates. The effective dose profile, which is defined as the convolution of the two-Gaussian kernel given by (2) and a design layout, for a rectangular pattern can be obtained as

$$\begin{aligned} D(x,y) = \frac{1}{4}&\left[\operatorname{erf}\left(\frac{x+d_x/2}{\alpha}\right) - \operatorname{erf}\left(\frac{x-d_x/2}{\alpha}\right)\right] \\ &\times\left[\operatorname{erf}\left(\frac{y+d_y/2}{\alpha}\right) - \operatorname{erf}\left(\frac{y-d_y/2}{\alpha}\right)\right] \\ +\frac{\eta}{4}&\left[\operatorname{erf}\left(\frac{x+d_x/2}{\beta}\right) - \operatorname{erf}\left(\frac{x-d_x/2}{\beta}\right)\right] \\ &\times\left[\operatorname{erf}\left(\frac{y+d_y/2}{\beta}\right) - \operatorname{erf}\left(\frac{y-d_y/2}{\beta}\right)\right], \end{aligned} \qquad (3)$$

where d_x and d_y denote the pattern sizes along x- and y-directions, respectively; we assume that the center of the rectangular pattern is located at the origin of the xy-plane. If we set $d_y = \infty$ in (3), the effective dose profile for an I/S pattern can be obtained as

$$D_{IS}(x)=\frac{1}{2}\left[\mathrm{erf}\left(\frac{x+d_x/2}{\alpha}\right)-\mathrm{erf}\left(\frac{x-d_x/2}{\alpha}\right)\right] \\ +\frac{\eta}{2}\left[\mathrm{erf}\left(\frac{x+d_x/2}{\beta}\right)-\mathrm{erf}\left(\frac{x-d_x/2}{\beta}\right)\right]. \tag{4}$$

And if d_y is chosen to be $d_y = d_x$, we get an effective dose profile along the x-axis for an I/C pattern as follows:

$$D_{IC}(x)=\frac{1}{2}\mathrm{erf}\left(\frac{d_x}{2\alpha}\right)\left[\mathrm{erf}\left(\frac{x+d_x/2}{\alpha}\right)-\mathrm{erf}\left(\frac{x-d_x/2}{\alpha}\right)\right] \\ +\frac{\eta}{2}\mathrm{erf}\left(\frac{d_x}{2\beta}\right)\left[\mathrm{erf}\left(\frac{x+d_x/2}{\beta}\right)-\mathrm{erf}\left(\frac{x-d_x/2}{\beta}\right)\right]. \tag{5}$$

The effective dose profiles for L/S and A/C patterns can also be obtained by locating isolated patterns at periodic positions and superposing the dose contributions from the individual isolated patterns. Under the assumption of the constant threshold model (CTM) with a threshold dose D_0, one can calculate the skew data, defined as the differences between measured CDs and design CDs, by solving the equations $D_{IS}(x_0) = D_0$ and $D_{IC}(x_0) = D_0$, numerically. Here, x_0 denotes the position where one of the pattern edges is determined using the CTM. Figure 3 shows an effective dose profile, edge positions of a designed pattern, and the relation between a threshold dose and the pattern edges defined by the CTM. According to the definition, the skew value is calculated as $Skew = 2x_0 - d_x$. If the skew value is much smaller than α and β, skew formulas for I/S and I/C patterns can be derived analytically using a Taylor expansion of the error function up to the 1st orders of the parameters $(x_0 - d_x/2)/\alpha$ and $(x_0 - d_x/2)/\beta$ as follows:

$$Skew_{IS}=\sqrt{\pi}\,\frac{\mathrm{erf}\left(\frac{d_x}{\alpha}\right)+\eta\,\mathrm{erf}\left(\frac{d_x}{\beta}\right)-2D_0}{\frac{1}{\alpha}\left[1-\exp\left(-\frac{d_x^2}{\alpha^2}\right)\right]+\frac{\eta}{\beta}\left[1-\exp\left(-\frac{d_x^2}{\beta^2}\right)\right]}, \tag{6}$$

$$Skew_{IC}= \\ \sqrt{\pi}\frac{\mathrm{erf}\left(\frac{d_x}{2\alpha}\right)\mathrm{erf}\left(\frac{d_x}{\alpha}\right)+\eta\,\mathrm{erf}\left(\frac{d_x}{2\beta}\right)\mathrm{erf}\left(\frac{d_x}{\beta}\right)-2D_0}{\frac{1}{\alpha}\mathrm{erf}\left(\frac{d_x}{2\alpha}\right)\left[1-\exp\left(-\frac{d_x^2}{\alpha^2}\right)\right]+\frac{\eta}{\beta}\mathrm{erf}\left(\frac{d_x}{2\beta}\right)\left[1-\exp\left(-\frac{d_x^2}{\beta^2}\right)\right]}. \tag{7}$$

If we set $\eta = 0$ in (6) and (7), the equations are reduced to analytical skew formulas for a one-Gaussian kernel.

We have fitted the analytical skew formulas (6) and (7) with experimental data for I/S and I/C patterns. Figures 4(a) and 4(b) show the fitted results for the cases of one- and two-Gaussian kernels, respectively. The fitting parameters were α = 0.2993 µm, D_0 = 0.4234 for Fig. 4(a), and α = 0.2794 µm, β = 1.3596 µm, η = 0.1218, D_0 = 0.4498 for Fig. 4(b). It seems that a one-Gaussian kernel is not enough to correctly represent the mask-making process and that at least a two-Gaussian kernel should be used in order to reproduce the experimental data for both the I/S and I/C patterns. We solved the CTM equations ($D_{IS}(x_0) = D_0$ and $D_{IC}(x_0) = D_0$) numerically and fitted the solved results with experimental skew data. The numerically obtained fitting parameters were α = 0.2779 µm, β = 1.3900 µm, η = 0.1240, and D_0 = 0.4500. The fitting parameters obtained using the analytical formulas (6) and (7) are in agreement with the numerically obtained ones within about 2%, which reveals the effectiveness of the analytical skew formulas for the two-Gaussian kernel presented in this section.

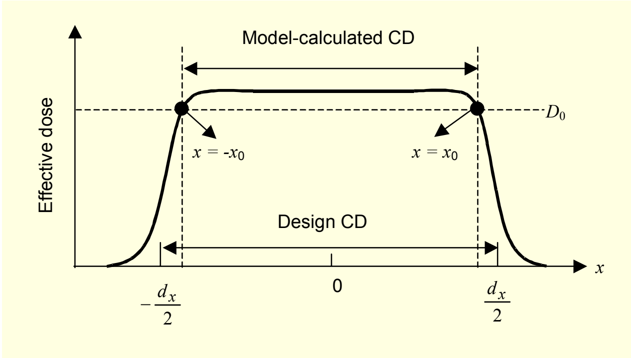

Fig. 3. An effective dose profile, edge positions ($x = -d_x/2$ and $d_x/2$) of a designed pattern and the relation between a threshold dose D_0, and the pattern edges ($x = -x_0$ and x_0) defined by the constant threshold model.

Figure 5 shows calculated and measured skew data for L/S, I/S, A/C and I/C patterns. The calculated data were obtained using the model parameters of α = 0.2794 µm, β = 1.3596 µm, η = 0.1218, and D_0 = 0.4498, which were the fitting parameters for Fig. 4(b). The calculated results, with the exception of the L/S patterns, are in good agreement with the measured results. The model parameters extracted in this section seem to satisfactorily represent the mask-making process for the patterns with lower pattern density than dense L/S patterns. It should be mentioned that we tried to obtain model parameters by fitting experimental skew data for all kinds of patterns (L/S, I/S, A/C and I/C) with model-calculated ones. The fitted results, however, were worse than those depicted in Fig. 5. The results showed a discrepancy between experimental and model-calculated data for all kinds of patterns, which implies that a complete representation of the mask-making process is inadequate even using the two-Gaussian kernel. We expect, however, that the two-Gaussian model investigated in this

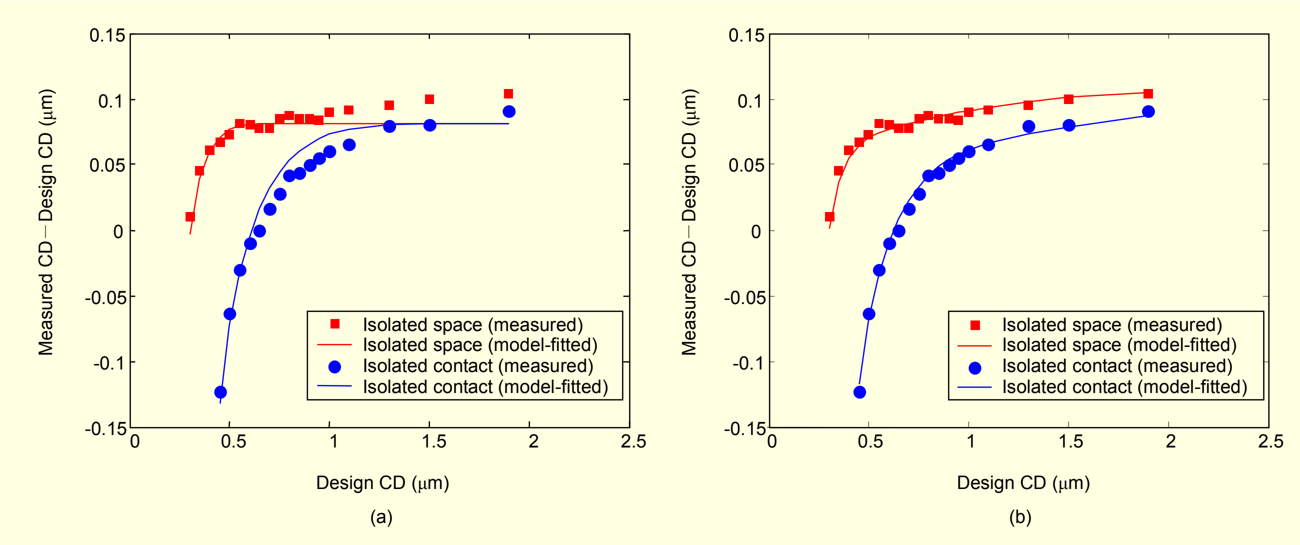

Fig. 4. Fitted results of experimental CD skew data for I/S and I/C patterns with analytical skew formulas derived from the models based on Gaussian kernels: (a) one-Gaussian kernel and (b) two-Gaussian kernel.

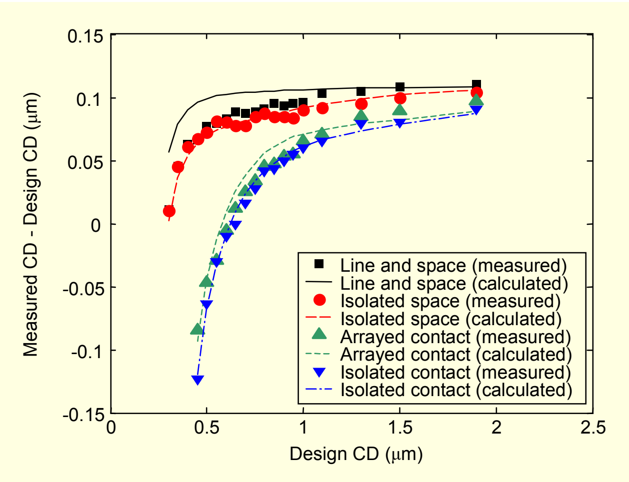

Fig. 5. Measured and calculated CD skew data. The calculated data were obtained with the two-Gaussian model parameters of $\alpha = 0.2794$ μm, $\beta = 1.3596$ μm, $\eta = 0.1218$ and $D_0 = 0.4498$.

paper can be usefully employed for mask-layers having patterns sparser than dense L/S patterns.

We tabulated bias rules for I/S, A/C and I/C patterns using the model parameters extracted by fitting the experimental skew data with (6) and (7). The results were in good agreement with those obtained by the method described in section II. In order to confirm the validity of the extracted model parameters, we compared the images of I/C patterns captured by a scanning electron microscope (SEM) with 2-dimensional pattern images predicted by the two-Gaussian model, as shown in Fig. 6. We can find that not only the pattern sizes but also the corner rounding characteristics for all CD sizes are reproduced perfectly by the two-Gaussian model. Now, we are trying to find a suitable kernel function for a complete representation of the mask-making process. As mentioned before, for the mask-making process considered in this paper, CD linearity is more dependent on pattern type than on pattern density. The inter-pattern proximity effect, i.e., the proximity effect induced by nearby patterns or pattern density, is mainly affected by the peripheral region of the kernel function. We therefore consider a truncated two-Gaussian kernel, which is defined by the product of a two-Gaussian function and a step function, as one of the promising kernel functions.

IV. Conclusion

In this paper, we have applied the PPC concept to a laser lithographic process used for the fabrication of photomasks. Bias rules were extracted by fitting the experimental CD linearity data with a nonlinear curve. An automated OPC tool was employed for rule-based LPC and a dramatic improvement of CD linearity was experimentally observed. A preliminary study on model-based LPC was executed using a two-Gaussian kernel. Analytical skew formulas for I/S and I/C patterns were introduced and model parameters were extracted by fitting the skew formulas with experimental data. We have observed that the model-predicted bias values were consistent with those obtained by the nonlinear curve-fitting method, and model-predicted pattern shapes for I/C patterns were in good agreement with the real pattern images captured by a SEM. The technical and theoretical approaches presented in this paper can provide useful information for further investigations on the PPC of photomask fabrication processes.

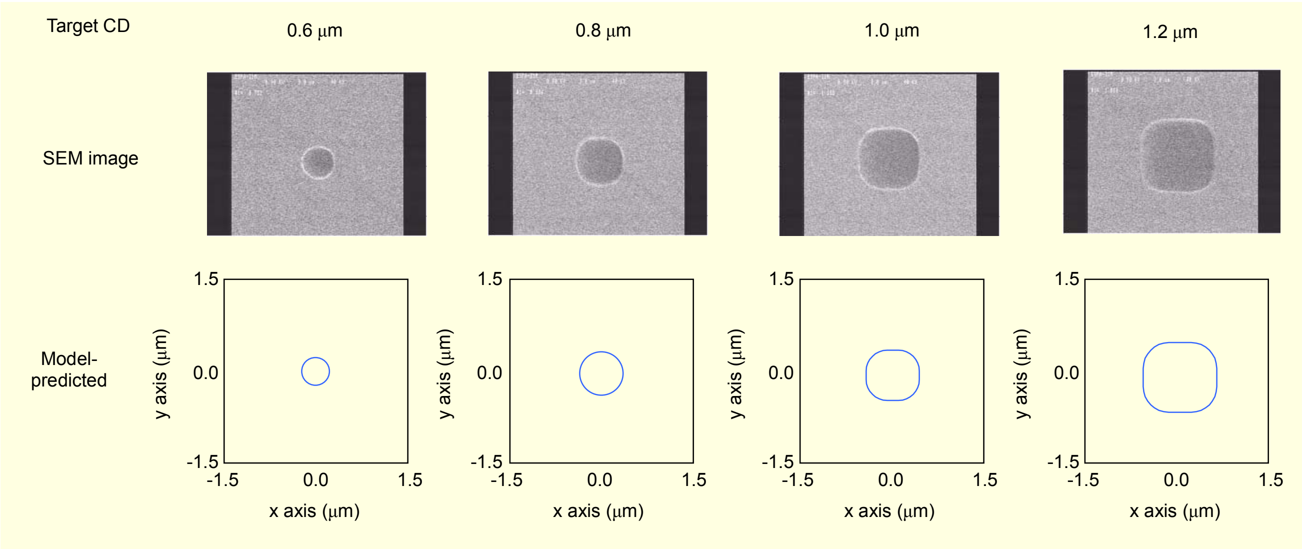

Fig. 6. Scanning electron microscope (SEM) images and model-predicted pattern shapes for isolated contact patterns.

Acknowledgment

One of the authors, Jong Rak Park, would like to thank J. B. Kim and S. U. Rhie of Synopsys, Inc., for their valuable discussions and advice.

References

[1] International Technology Roadmap for Semiconductors (ITRS) 2003, http://public.itrs.net/.

[2] H.-K. Oh, "Process Study of a 200 nm Laser Pattern Generator," *J. Korean Phys. Soc.*, vol. 41, no. 6, Dec. 2002, pp. 839-842.

[3] Y. Sato, H. Handa, Y. Kushida, S. Asai, H. Maruyama, Y. Miyahara, M. Naitoh, R. Hikichi, Y. Kawasaki, H. Miyashita, and S. Noguchi, "Process Bias Control with Thin Cr Film Blanks for 90 nm-node Reticle Fabrication," *Proc. SPIE*, vol. 4889, 2002, p. 50.

[4] A.K. Wong, *Resolution Enhancement Techniques in Optical Lithography*, SPIE Press, Bellingham, 2001.

[5] J.-S. Kim, K.-C. Park, Y.-D. Kim, Y.-H. Oh, J.-C. Lee, C.S. Go, and S. Lim, "Monte-Carlo Based Optical Proximity Correction of DRAM Storage Capacitors and Hammer Heads," *J. Korean Phys. Soc.*, vol. 40, no. 1, Jan. 2002, pp. 163-166.

[6] E.-J. Seo, H.-J. Bak, S.-K. Kim, Y.-S. Sohn, and H.-K. Oh, "Modification of the Development Parameter for a Chemically Amplified Resist Simulator," *J. Korean Phys. Soc.*, vol. 40, no. 4, Apr. 2002, pp. 725-728.

[7] S.-K. Kim and H.-K. Oh, "Bulk Image Formation of Scalar Modeling in a Photoresist," *J. Korean Phys. Soc.*, vol. 41, no. 4, Oct. 2002, pp. 456-460.

[8] W. Maurer, C. Dolainsky, J. Thiele, C. Friedrich, and P. Karakatsanis, "Process Proximity Correction Using an Automated Software Tool," *Proc. SPIE*, vol. 3334, 1998, p. 245.

[9] P. van Adrichem, *Loading Effect Correction with CATS: An Application Note*, Synopsys, Inc., Mountain View, 2003.

[10] D. Kim, B. Kim, and G-T. Park, "A Plasma-Etching Process Modeling Via a Polynomial Neural Network," *ETRI J.*, vol. 26, no. 4, Aug. 2004, pp. 297-306.

[11] H.-B. Kim, W.-K. Ma, C.-N. Ahn, and K.-S. Shin, "Optical Lithography Simulation Considering Impact of Mask Errors," *Proc. SPIE*, vol. 4691, 2002, p. 1278.

Jong Rak Park received the PhD degree in physics from Korea Advanced Institute of Science and Technology (KAIST), Daejon, Korea, in 2000. His dissertation work involved diode-pumped solid-state lasers for optical frequency standards and quantum-optical investigations on atom-photon interactions. In 2000, he joined the Department of Optoelectronic Materials, Research Laboratory, LG Cable Co., Ltd., Anyang, Gyeonggi-do, Korea, where he was engaged in the research and development of various functional optical films and cholesteric liquid crystal (CLC) polarizers for liquid crystal displays (LCDs). In 2001, he joined the Semiconductor R&D Division, Samsung Electronics Co., Ltd., Yongin, Gyeonggi-do, Korea, where he was involved in the research and development of lithographic techniques including optical projection lithography for semiconductor devices and e-beam and laser direct writing for photomasks. Since 2003, he has been an Assistant Professor with the Department of Photonic Engineering, Chosun University, Gwangju, Korea. His research interests include the fundamentals and applications of laser optics and applications of optical techniques to manufacturing processes of semiconductor devices and LCDs.

Hyun Su Kim received the BS degree in physics from Sogang University, Seoul, Korea, in 1990 and the MS and PhD degrees in physics from Korea Advanced Institute of Science and Technology (KAIST), Daejeon, Korea, in 1992 and 1998. His dissertation work involved an Nd liquid laser amplifier and an Nd glass laser oscillator with a stimulated Brillouin scattering mirror. In 1998, he joined the laboratory for Quantum Optics, Korea Atomic Energy Research Institute (KAERI), where he had been engaged in the research and development of diode-pumped solid-state lasers and dye lasers. Since 2002, he has been an Assistant Professor with the Department of Photonic Engineering, Chosun University, Gwangju, Korea. His research interests include bio-optics, ultra-short pulse laser applications, and passive light modulators with semiconductor quantum well structure.

Jin-Tae Kim received the BS and MS degrees from Korea University, Seoul, Korea, in 1984 and 1986, and the PhD degree from the University of Iowa, Iowa City, USA in 1995, all in physics. His dissertation work involved all-optical multiple resonance spectroscopy of the potassium diatomic molecule using a high resolution CW ring dye/Ti:sapphire laser. In 1995, he joined the Physics Department, University of Connecticut, Storrs, where he performed laser molecular supersonic beam experiments for hydrogen molecules. In 1997, he joined the laboratory for Quantum Optics, Korea Atomic Energy Research Institute, where he was engaged in the research and development of dye lasers and laser atomic spectroscopy by using a time of mass spectrometer. He is now an Assistant Professor with the Department of Photonic Engineering, Chosun University, Gwangju, Korea. His research interests include laser applications such as surface profile measurements using the interferometer, laser welding, ultra-sensitive detection of gas, and laser atomic and molecular spectroscopy.

Moon-Gyu Sung received the MS degree in physics from Hanyang University, Seoul, Korea, in 2000. Since 2000, he has been an Engineer with Semiconductor R&D Division, Samsung Electronics Co., Ltd., Yongin, Gyeonggi-do, Korea. His work is focused on the production and repair of photomasks for semiconductor device manufacturing.

Won-Il Cho received the MS degree in physics from Sogang University, Seoul, Korea, in 2000. Since 2000, he has been an Engineer with Semiconductor R&D Division, Samsung Electronics Co., Ltd., Yongin, Gyeonggi-do, Korea. His work is focused on the production and inspection of photomasks for semiconductor device manufacturing.

Ji-Hyun Choi received the BS degree in mathematics from Inha University, Incheon, Korea in 1994. Since 1994, she has been working with Semiconductor R&D Division, Samsung Electronics Co., Ltd., Yongin, Gyeonggi-do, Korea. She has been engaged in the research and development of photomask technology for next-generation semiconductor devices. Now, she is a Senior Engineer with Photomask Team, Semiconductor R&D Division, Samsung Electronics.

Sung-Woon Choi received the BS and MS degrees from Korea University, Seoul, Korea in 1986 and 1991, all in physics. Since 1991, he has been working with Semiconductor R&D Division, Samsung Electronics Co., Ltd., Yongin, Gyeonggi-do, Korea. Now, he is a Principal Engineer of Photomask Team, Semiconductor R&D Division, Samsung Electronics, where he is in charge of the research and development of current and next-generation photomask technologies.